Imaging Neuroscience
an open access journal

Research Article

Structural projections to the nucleus accumbens link to impulsive components of human risk preference

Loreen Tisdall[a], Kelly MacNiven[b], Josiah Leong[c], Renato Frey[d], Jörg Rieskamp[e], Ralph Hertwig[f], Brian Knutson[b], Rui Mata[a]

[a]Center for Cognitive and Decision Sciences, University of Basel, Basel, Switzerland
[b]Department of Psychology, Stanford University, Stanford, CA, United States
[c]Department of Psychological Science, University of Arkansas, Fayetteville, AR, United States
[d]Cognitive and Behavioral Decision Research, University of Zurich, Zürich, Switzerland
[e]Center for Economic Psychology, University of Basel, Basel, Switzerland
[f]Center for Adaptive Rationality, Max Planck Institute for Human Development, Berlin, Germany

Corresponding Author: Loreen Tisdall (loreen.tisdall@unibas.ch)

ABSTRACT

Functional responses in the Nucleus Accumbens (NAcc) to risk- and reward-related cues can predict real-life risk-taking behavior. Since NAcc activity depends on neurotransmission from connected brain regions, projections to the NAcc may also predict risk preference. To quantify risk preference, we employed latent variables previously derived in a comprehensive, independent study examining the psychometric structure of risk preference, which yielded a general risk preference factor as well as several specific factors, including a factor capturing impulsivity. Informed by previous work, we preregistered a set of hypotheses concerning the association between different risk preference factors and fractional anisotropy (or FA, which is sensitive to fiber coherence) for projections to the NAcc from Medial PreFrontal Cortex (MPFC), Anterior Insula, Amygdala, and an inferior tract from the Ventral Tegmental Area (iVTA). We tested our hypotheses in a community sample of 125 healthy human adults. As predicted, bilateral iVTA-NAcc tract FA showed a negative correlation with a psychometric factor that captured impulsivity, generalizing findings from prior research. Also as predicted, FA of the bilateral Amygdala-NAcc tract was positively associated with the impulsivity factor. Contrary to predictions, however, we observed no robust associations between the general risk preference factor and FA for projections from bilateral MPFC, right Anterior Insula, or bilateral Amygdala to the NAcc. Notably, exploratory unilateral analyses revealed an association between the general risk preference factor and left MPFC-NAcc tract FA. Taken together, these findings suggest that impulse control as a facet of risk preference maps onto specific neurobiological targets, while more general facets of risk preference may be supported by structural properties of lateral fronto-striatal projections. Although the exact associated functional mechanisms remain to be fully clarified, conNAcctomic approaches like the one presented here could pave the way for further research into the physiological foundations of risk preference and related constructs.

Keywords: risk, reward, impulsivity, psychometric modeling, tractography, diffusion-weighted imaging

1. INTRODUCTION

Decisions shape the start, course, and end of our lives. While some decision scenarios are well defined and lead to trivial choices, others involve choosing between multiple uncertain, potentially consequential alternatives, that is, they involve risk (Aven, 2012; Schonberg et al., 2011). Risk preference—the tendency to engage in potentially rewarding activities that have a probability of harm or loss

Received: 7 December 2023 Revision: 14 August 2024 Accepted: 25 September 2024 Available Online: 16 October 2024

(Nigg, 2017)—and its underlying psychological traits are thought to be consequential for many domains of life, including wealth, health, criminal activity, and overall well-being (Moffitt et al., 2011; Steinberg, 2013). Risk preference, thus, presents a desirable target for intervention (Conrod et al., 2013), with debates about the nature of risk and the determinants of individuals' risk propensity unfolding in various disciplines, including psychology, economics, and biology (Bernoulli, 1954; Mata et al., 2018; Mishra, 2014; Slovic, 1964).

Recent multivariate genetic analyses have started to examine potential biological pathways, showing that genetic differences can explain common variance in risk preference, and, importantly, that genetic differences are predominantly expressed in brain tissue (Karlsson Linnér et al., 2021). Honing in on specific neural targets, empirical studies suggested that functional activation in the nucleus accumbens (NAcc) in response to reward and risk-related cues can predict real-life risk taking (Leong et al., 2016; Sherman et al., 2018), and, in a more applied context, drug-cue-related NAcc activation has been shown to predict relapse to stimulant use disorder (MacNiven et al., 2018). Comparative animal studies (Haber & Knutson, 2010) as well as human anatomical research (Cartmell et al., 2019) have demonstrated that the NAcc is a highly connected brain region, leading to the general question whether characteristics of tracts projecting to and modulating signal in the NAcc—which we collectively refer to as the conNAcctome (Tisdall et al., 2022)—may be associated with individual differences in risk preference. The conNAcctome encompasses dopaminergic and glutamatergic tracts converging on the NAcc from the Medial Prefrontal Cortex (MPFC), Anterior Insula (AIns), Amygdala (Amy), and a tract from the Ventral Tegmental Area traversing below the Anterior Commissure (iVTA). Speaking to the importance of a conNAcctomic approach, dysregulation within ascending dopaminergic projections from the midbrain to the striatum due to reduced dopamine autoreceptor availability, for example, has been demonstrated to account for individual differences in impulsivity (Buckholtz et al., 2010).

Until recently, studying these tracts involved invasive methods (Chung & Deisseroth, 2013; Jbabdi et al., 2013; Leuze et al., 2021) unsuitable for most human research, but Diffusion-weighted Magnetic Resonance Imaging (DMRI) offers a noninvasive method to reliably reconstruct and characterize these projections in vivo (Alexander et al., 2019; Kai et al., 2022; Lazari & Lipp, 2021). DMRI involves modeling and quantifying the diffusivity (i.e., directedness) of water molecules in the brain which may support inferences about the structure of underlying fiber bundles. Diffusion is traditionally summarized by standard yet distinct metrics, including fractional anisotropy (FA) and radial diffusivity (RD) (Lazari & Lipp, 2021; Suchting et al., 2021). In animal models, the reduction of lipids has been shown to causally and predictably influence DMRI metrics (e.g., lower FA and higher RD; Janve et al., 2013; Leuze et al., 2017; Ou et al., 2009; Song et al., 2002), suggesting that these metrics can partially index myelination or lipid coherence. FA has, thus, commonly been used as an index that is sensitive to fiber coherence, with higher coherence implying more effective signal transmission between regions. In turn, RD (and its inverse) has also been linked to varying microstructural tissue properties, including axon myelination (Beard et al., 2019; Janve et al., 2013; Song et al., 2002), fiber spread (Choe et al., 2012), and cell and axon density (Stolp et al., 2018).

The literature on DMRI approaches offers strong support for the contribution of conNAcctome tracts to risk-related phenotypes. For example, reduced FA in fronto-limbic white matter was associated with future risk taking in substance-using adolescents (Morales et al., 2020). Moreover, right AIns-NAcc tract FA has been associated with incentivized inhibition (Leong et al., 2018) and preference for skewed gambles (Leong et al., 2016), and was predictive of relapse to stimulant drug use (Tisdall et al., 2022). Furthermore, projections from the Amygdala have been suggested to be associated with risk tolerance (Jung et al., 2018). Finally, reduced FA of the iVTA-NAcc tract has been shown to be associated with impulsivity (MacNiven et al., 2020) and with stimulant use disorder diagnosis but not relapse (MacNiven et al., 2020; Tisdall et al., 2022).

Although these recent findings offer novel insights and, importantly, may pave the way for intervention and prevention efforts (Poldrack et al., 2018; Shivacharan et al., 2022), one remaining challenge to progress stems from the diversity of existing research when it comes to assessing risk preferences. In practice, researchers adopt different methods to capture individual differences in risk preference: self-report measures have a long tradition in psychological research (Krosnick et al., 2005), and are used to capture stated preferences (Frey et al., 2021; Mata et al., 2018), while behavioral measures with firm roots in economics reveal preferences from gamified, lottery-type tasks (Appelt et al., 2011; Beshears et al., 2009; Charness et al., 2013; Frey et al., 2021; Mata et al., 2018). In practice, different measures have repeatedly been shown to be not or only weakly correlated, with particularly behavioral measures of risk preference and related constructs showing low convergence (Frey et al., 2017, 2021; Mamerow et al., 2016; Mata et al., 2011, 2018; Pedroni et al., 2017). As such, we would expect the results of studies probing the link between brain tract structure and risk preference to vary as a function of how

risk preference was operationalized. This makes the identification of reliable neural targets for intervention a challenging endeavor.

In this study, we aimed to tackle the issue of measurement plurality and the resulting divergence of brain-outcome associations. Specifically, we aimed to avoid biased estimates stemming from the use of single measures of risk preference by employing risk preference factors as our outcome variables. These factors were derived independently through psychometric modeling based on 39 risk-taking measures collected in a sample of over 1500 young adults (Frey et al., 2017). Combining psychometric risk preference factors with a conNAcctomic approach, our goal was to examine whether coherence-sensitive DMRI metrics of specific brain tracts relate to individual differences in risk preference.

Recent work (Marek et al., 2022) has suggested that when searching brainwide for brain-behavior associations, a sample size of hundreds or thousands of participants is required to establish robust associations, and relevant genetic associations for risk-related outcomes (Aydogan et al., 2021) have been reported for very large datasets. Sample size is of critical importance for the internal validity of a study, primarily through its impact on the reliability and precision of the results, as well as the ability to detect true effects. In this study, we sought to increase internal validity by (a) carefully selecting brain and behavioral indices with moderate to high test-retest reliability (cf. section 2), (b) focusing on a small, a priori defined set of brain regions previously implicated in the outcomes under investigation, and (c) exhaustively controlling for confounds. In addition, we preregistered a set of hypotheses concerning the associations between brain tract structure and risk preference factors (Table 1).

We based our hypotheses on not only previous empirical findings but also mechanistic explanations, including the idea that decreased FA between the right AIns and NAcc might result in the decreased dampening of NAcc-related reward signal as a function of an affective inhibitory signal originating in AIns (Leong et al., 2016, 2018). For example, we predicted a negative association between a general risk preference factor (R) and bilateral MPFC-NAcc FA (H1), and with right AIns-NAcc FA (H2). We also predicted an association between R and bilateral Amy-NAcc FA (H3), but tested a bidirectional hypothesis due to the heterogeneity of previous findings. For F4, a factor capturing impulsivity, we predicted a positive association with bilateral Amy-NAcc FA (H4) but a negative association with bilateral iVTA-NAcc FA (H5).

Table 1. Research hypotheses for associations between risk preference and conNAcctome structure (FA and 1/RD).

H	Factor	Tract (hemisphere)	Predicted association	Selected source for prediction
1	R	MPFC-NAcc (lr)	–	Morales et al. (2020)
2	R	AIns-NAcc (r)	–	Leong et al. (2016, 2018)
3	R	Amy-NAcc (lr)	±	Cohen et al. (2009); Jung et al. (2018)
4	F4	Amy-NAcc (lr)	+	van den Bos et al. (2014)
5	F4	iVTA-NAcc (lr)	–	MacNiven et al. (2020)

Note. H = Hypothesis; r = right; lr = bilateral.

2. METHOD

The study was reviewed and approved by the German Society for Psychology, and the Ethics Committee of the Max Planck Institute for Human Development. All methods were carried out in accordance with the relevant guidelines and regulations. Prior to participation in the study, all individuals gave written informed consent. The analyses were preregistered on AsPredicted (https://aspredicted.org/bx49i.pdf).

2.1. Participants

The participants in this neuroimaging study were recruited from an existing pool of individuals who had taken part in the Basel-Berlin Risk Study (BBRS). The overarching aim of the BBRS is to examine the psychometric structure and biological underpinnings of risk preference in a large sample (N = 1507) of young human adults (Dutilh et al., 2017; Frey et al., 2017; Pedroni et al., 2017; Tisdall et al., 2022). Participation in the BBRS involves completion of a laboratory session, during which individuals are assessed on a large battery of behavioral and self-reported risk-taking measures, as well as on other individual differences measures, including cognitive capacity, personality, affect, and genetics. Further details and summaries of all BBRS sub-samples and measures are reported on the BBRS OSF repository (https://osf.io/rce7g). The BBRS was run in Basel (Switzerland) and in Berlin (Germany); for this study we only recruited individuals from the Berlin site due to the location of the scanning facilities available. Exclusion criteria for participation were any contraindications with regards to magnetic resonance imaging (MRI) safety (e.g., safety-limiting non-removable implants), a history of neurological or psychiatric conditions, reported use of psychoactive medication or substances, and concurrent psychiatric treatment.

To compensate for participant exclusions (e.g., due to excessive head motion in the scanner, image artifacts),

we recruited a total of 133 participants to achieve a minimum effective sample size of N ~ 100 participants (Yarkoni, 2009). Two participants aborted the scanning session before any MRI data were collected; these two participants were removed from all subsequent analyses. A further five participants were excluded because the critical diffusion-weighted imaging sequence necessary for this project was not collected due to time constraints, and one additional participant was excluded due to incidental anatomical findings. After exclusions, all analyses included a sample of 125 young adult human participants comprising 67 (53.6%) females, with a sample mean age of 25.19 years (SD = 2.57, range = 20.4–30.1 years).

2.2. Study protocol

We contacted individuals who had previously completed the BBRS laboratory session by phone and invited them to a follow-up neuroimaging study. Interested individuals were initially screened for any MRI-safety contraindications prior to being enrolled in the study, and again on the day of the MRI session. All participants provided written informed consent. Participants were then scanned using MRI to acquire anatomical and diffusion-weighted images. We also collected functional scans, but these do not contribute to the current analyses and are not described further (cf. Tisdall et al., 2020). Due to the fact that participants in the MRI session were scanned at different intervals after completing the laboratory component (median interval = 6.28 months, mean interval = 6.63 months, SD = 3.99 months, range = 1–453 days), we performed supplementary robustness checks to control for interval.

After scanning, participants completed a demographic questionnaire as well as additional measures that we do not focus on in the current analyses. Participants received a base payment of 25 Euro for their participation. In addition, participants could increase their earnings based on their decision making in the two functional MRI tasks. All participants were informed about the incentive structure and received cash earnings at the end of the session (mean total earnings = 41.50 Euro, SD = 14.50 Euro).

2.3. Risk preference factors

The quantification of risk preference based on single risk-taking measures, in particular behavioral measures, runs into problems of validity, reliability, and convergence (Enkavi et al., 2019; Frey et al., 2017; Pedroni et al., 2017). To address these issues, we used risk preference factors as outcome variables that had previously and independently been derived from the psychometric modeling of 39 risk-taking measures collected in the full BBRS sample (Frey et al., 2017). Notably, the BBRS included three broad categories of measures, namely propensity, frequency, and behavioral measures; see Supplementary Methods and Table S1 for details concerning specific risk preference measures and the adopted bifactor model. The implemented bifactor model extracted a general risk preference factor, R, and seven orthogonal specific factors which captured additional domain- or situation-specific variance. These domain-specific factors were thought to capture attitudes and behaviors associated with health risk taking (F1), financial risk taking (F2), recreational risk taking (F3), impulsivity (F4), traffic risk taking (F5), occupational risk taking (F6), and choices in (monetary) lotteries (F7).

Test–retest reliability for the psychometric factors (assessed in a sub-sample of 106 BBRS laboratory participants) was shown to be higher than for any of the behavioral measures; for example, R had a 6-month retest reliability of 0.85, whereas many of the behavioral measures tested yielded retest reliabilities below 0.5. In this study, we focused on factors with test-retest reliabilities above 0.5, that is, R and all domain-specific factors except F7. Our main hypotheses concerned R (test-retest correlation $r = 0.85$) and the impulsivity-capturing factor F4 (test-retest correlation $r = 0.7$), but we also conducted exploratory analyses on the remaining domain-specific factors. Factor values for the current MRI sample were approximately normally distributed (Fig. 1, panel A; Supplementary Materials) and mainly orthogonal (Fig. 1, panel B).

2.4. Scan acquisition

Neuroimaging data were collected at the MRI Laboratory at the Max Planck Institute for Human Development (Berlin, Germany) on a 3T Siemens MRI system with a 12-channel head coil. For the DMRI, we used a single-shot echo-planar imaging sequence with the following parameters: b = 1000 s/mm^2, 61 diffusion directions, TR = 10 s, TE = 94 ms, fat saturated flip angle = 110°, FOV = 208 mm x 208 mm, 69 axial slices, and voxel dimensions = 2.0 mm isotropic. At the beginning of the DMRI scan, we acquired eight non-diffusion weighted images (b = 0 s/mm^2). A structural T1-weighted scan was acquired for every participant at the start of the MRI session via a magnetization-prepared rapid gradient echo sequence (repetition time = 2500 ms, echo time = 4.77 ms, inversion time = 1100 ms, flip angle = 7°, FOV = 256 mm × 256 mm, 192 slices, voxel dimensions = 1.0 mm isotropic).

2.5. ConNAcctome volumes of interest (VOI)

We focused on four tracts projecting to the NAcc (Fig. 2), namely from the MPFC, AIns, Amy, and Ventral Tegmental

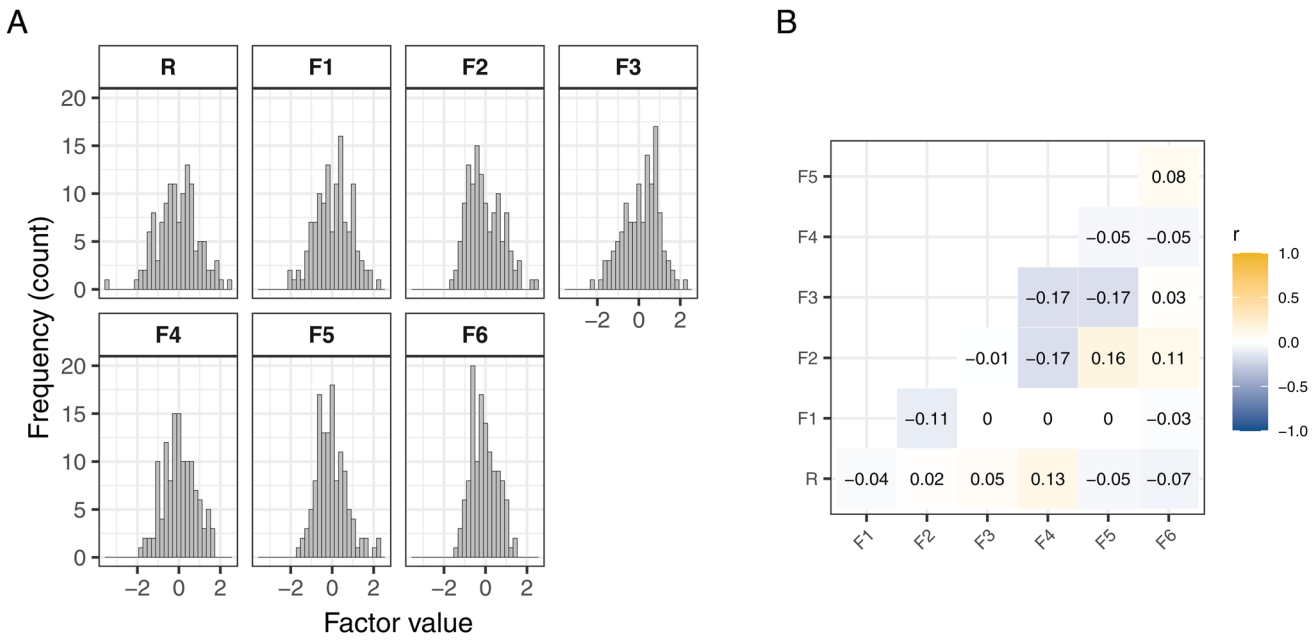

Fig. 1. Risk preference factors. (A) Distribution of the general and domain-specific risk preference factors. (B) Correlation analyses between the psychometric factors for the MRI sub-sample of the BBRS (N = 125) confirms orthogonality between the factors. R = General, F1 = Health, F2 = Financial, F3 = Recreational, F4 = Impulsivity, F5 = Traffic, F6 = Occupational.

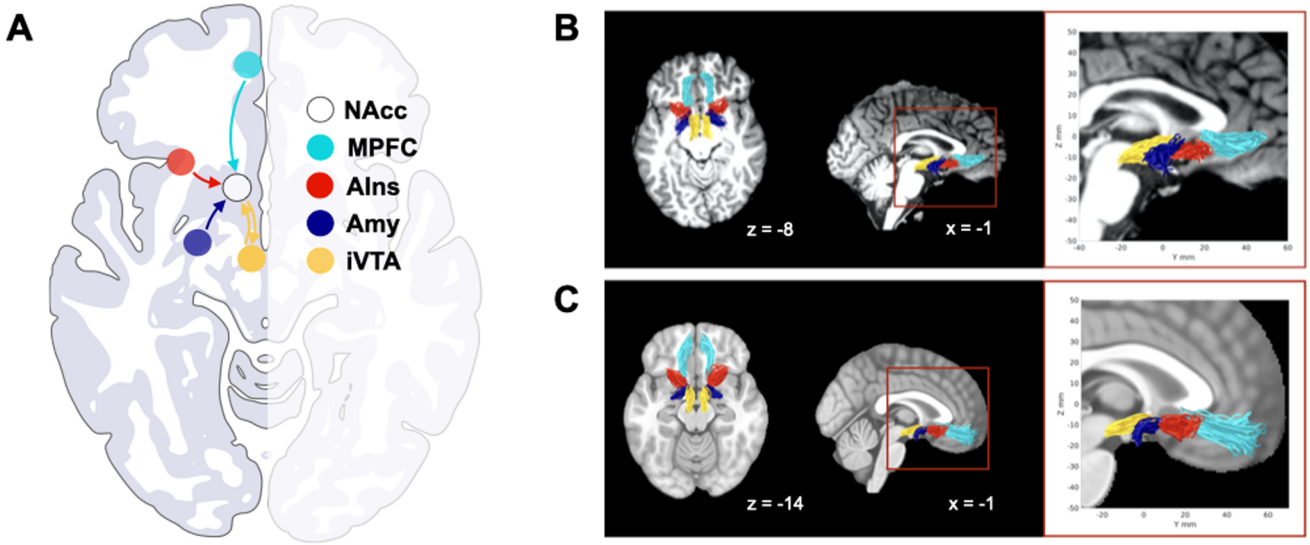

Fig. 2. ConNAcctome tracts. (A) Schematic with previously demonstrated directionality of projections. (B) Tracts in a representative subject's AC-PC aligned native brain space. (C) Group tract templates in MNI space.

Area (VTA) (Haber & Knutson, 2010). For the seed-based tractography in individuals' native space, we defined the NAcc, AIns, and Amy VOIs based on automated tissue segmentation and parcellation using FreeSurfer (Leong et al., 2016, 2018; MacNiven et al., 2020; Tisdall et al., 2022), and the MPFC and VTA VOIs were defined based on previously reported methods (Leong et al., 2016; MacNiven et al., 2020; Samanez-Larkin et al., 2012; Tisdall et al., 2022). We also created a native space white matter mask for every participant (using FreeSurfer); this was used to restrict tractography to white matter voxels. Previous work suggested anatomically-specific associations between impulsivity and a VTA tract traversing below (versus above) the Anterior Commissure (AC) (MacNiven et al., 2020; Tisdall et al., 2022). To examine this specificity, we performed tractography for the VTA-NAcc tract using an exclusionary mask at the AC and thereby isolated separate fiber bundles projecting from the VTA to the NAcc,

which run below and above the AC. This allowed us to separately characterize the superior and inferior VTA (iVTA) tracts, and examine their association with impulsivity. In our schematic of the conNAcctome (Fig. 2, panel A), we include directional pathways between brain regions. While the current approach using diffusion MRI cannot resolve directionality, comparative work (e.g., using tracer studies) has enabled identification of afferent and efferent connections within the reward circuitry (Haber & Knutson, 2010). Thus, our schematic incorporates these insights.

2.6. DMRI data preprocessing and tractography

The raw DMRI data were preprocessed using the open-source software package mrDiffusion (www.github.com/vistalab/vistasoft), which we ran in MATLAB R2016b. As described in (MacNiven et al., 2020; Tisdall et al., 2022), preprocessing included motion correction, registration of each diffusion-weighted image to the mean of the non-diffusion weighted (b = 0) images, co-registration of the mean of the non-diffusion weighted (b = 0) images to the T1-weighted volumes, and resampling of the raw diffusion-weighted images to 2 mm isotropic voxels (Ashburner & Friston, 2005). Using least-squares error minimization, we fit tensors to the diffusion measurements in each voxel. From each voxel's tensor, we then created voxel-wise maps of Fractional Anisotropy (FA), Mean Diffusivity (MD), Radial Diffusivity (RD), and Axial Diffusivity (AD). To precisely identify and characterize the conNAcctome tracts, we combined probabilistic tractography in individuals' native space with constrained spherical deconvolution using MRtrix (v3.0) (Tournier et al., 2007). Application of a constrained spherical deconvolution model of water diffusion allowed us to model crossing fibers. In a first step, we fit a model with a maximum harmonic envelope of 8 to estimate the Fiber Orientation Distribution (FOD) within each voxel. In a second step, we tracked fiber pathways between the seed VOIs and the NAcc, using the FOD as a probability density function (in each voxel). The tractography was performed using the following parameters: desired number of fibers = 1000; maximum number of attempted fibers = 107; algorithm, iFOD2; and FOD cutoff = 0.05. Using participants' white matter masks, tractography was restricted to white matter voxels only. The reconstructed fiber groups were subsequently cleaned with Automated Fiber Quantification (Yeatman, Dougherty, Myall, et al., 2012). For this, fiber groups were resampled to 100 equidistant nodes between the seed and NAcc VOIs. We then calculated the core of the fiber group as the mean coordinates at each of the 100 nodes. Fibers with coordinates that fell more than three standard deviations from the core coordinates of the fiber group (via computation of the Mahalanobis distance) were excluded from the fiber group, as were fibers with a length more than two standard deviations from the mean length of the fiber group. Cleaning was performed in an iterative fashion with a maximum of five iterations. To compare fiber density maps across subjects in tract segmentation analyses, each subject's anatomical image was spatially normalized to a group template (TT_N27) using a non-linear registration method with ANTS software (Avants et al., 2014).

2.7. DMRI metrics

Our statistical analyses targeted FA and RD; for ease of interpretation, we calculated the inverse of RD (1/RD) to align with the notion of a higher metric being indicative of more fiber coherence (cf. Supplementary Materials for further details). Initial plotting of node-wise FA and 1/RD for all 125 participants identified one participant with outlier tract metrics for the MPFC-NAcc tract (cf. Supplementary Materials for further details on outlier detection); we excluded this particular participant from analyses involving the MPFC-NAcc tract. Critically, extant work conducted by the current authors as well as external researchers (Kruper et al., 2021; Rokem et al., 2015; Tisdall et al., 2022) suggests that diffusion metrics show moderate to (very) high reliability, thus reducing measurement error and contributing to internal validity.

2.8. Analysis protocol for individual differences analyses

Our analyses targeted out-of session associations between psychometric risk preference factors and structural projections. Following previously established analytical routines (Tisdall et al., 2022), we adopted the following order of analytical procedures to test our hypotheses.

First, for every hypothesis, we followed previously described methods (Nichols & Holmes, 2002) and adopted a linear regression-based permutation test approach to establish the required number of consecutive nodes along a given tract for an association to be significant at $p < 0.05$ (corrected for multiple testing along a tract of 100 nodes). This approach is comparable to computing a cluster extent for functional MRI analyses.

Second, we used linear regression analysis to identify all nodes along a given tract which showed an association at $p < 0.05$ (uncorrected) with the specific risk preference factor of interest, and compared the number of observed consecutively significant nodes with the number of required consecutively significant nodes.

Third, for the purpose of model comparison, for every node cluster that met or exceeded the required number of consecutively significant nodes, we calculated a

tract-specific summary FA (or 1/RD) metric on the basis of a simple average over all observed consecutively significant nodes, and used this summary tract metric in multiple linear regression analyses. We note that analyses using summary tract metrics are not independent because the selection of nodes is informed by the results from the node-wise analyses (Vul & Pashler, 2012), hence they do not provide unbiased estimates. However, these analyses do not challenge the main (node-wise) results, and facilitate both controlling for confounds and comparison with previous work. All regression analyses were based on standardized and residualized (with regards to age and gender) risk preference factor values, as well as standardized summary tract metrics to facilitate effect comparison across tracts.

Fourth, to estimate and visualize the association between tract metrics and risk preference factors while exhaustively controlling for the influence of demographic (age, gender) and methodological (i.e., number of streamlines) variables, we adopted a multiverse approach (Steegen et al., 2016) to data analysis by performing specification curve analysis (Frey et al., 2021; Simonsohn et al., 2020) using the summary tract metrics (cf. Supplementary Materials for details). We followed up on the main analyses with exploratory analyses aimed at examining potential laterality effects, and to pinpoint additional associations which may be targeted more directly in future studies.

3. RESULTS

3.1. ConNAcctome tracts

We successfully tracked and characterized all tracts bilaterally in all subjects. Figure 2, panel B shows the conNAcctome tracts in an individual's AC-PC aligned native brain space, illustrating the anterior-to-posterior location of the tract endpoints in the NAcc originating in the MPFC, AIns, Amy, and iVTA, respectively. To visualize and qualitatively compare tract locations across subjects, for each tract we generated group templates in standard MNI space (Fig. 2, panel C). The MNI group tracts suggest a high degree of similarity across subjects concerning the location of conNAcctome tracts in both hemispheres. We plotted sample and individual tract profiles for FA and 1/RD separately for the two hemispheres of each tract (Fig. S1). As described previously (Yeatman, Dougherty, Ben-Shachar, & Wandell, 2012), tract metric profiles were heterogeneous across tracts, but comparatively more homogeneous across hemispheres.

3.2. Risk preference as a function of tract metrics

3.2.1. Node-wise associations

For our main individual differences analyses, we followed a permutation-based approach to evaluate node-wise associations between tract metrics and risk preference factors while controlling for multiple comparisons (see Methods for details). As predicted, FA of the Amy-NAcc tract (bilateral) was positively associated with F4 (Table 2; Fig. 3, panel A); this result was specific to FA and did not extend to 1/RD (Table S2; Fig. S4). Also as predicted, we observed a negative association between the impulsivity-capturing factor F4 and FA in an extended cluster of nodes along the bilateral iVTA-NAcc tract (Table 2; Fig. 3, panel B). This association was also observed for 1/RD (Table S2; Fig. S4).

Although we identified node clusters in bilateral MPFC-NAcc and right AIns-NAcc associated with the general risk preference factor R (Fig. S4), the extent of these clusters did not meet the required threshold, and the observed associations were contrary to the predicted directions. Contrary to our predictions, we found no association between the general risk preference factor R and Amy-NAcc FA or 1/RD (Table 2; Table S2).

3.2.2. Model comparison

To examine the robustness of the observed brain-behavior associations, we performed a set of model comparisons. For this purpose, we generated summary tract metrics for the bilateral Amy-NAcc and iVTA-NAcc tracts, by averaging FA metrics across the consecutive nodes found to be significantly associated with the impulsivity-capturing factor F4 (cf. 'Nodes' column in

Table 2. Node-wise regression results for FA, organized by hypothesis.

H	Factor	Tract (hemisphere)	# Observed/# required	Nodes	Predicted direction	Observed direction
1	R	MPFC-NAcc (lr)	16/27	27–42	–	+
2	R	AIns-NAcc (r)	10/25	33–42	–	+
3	R	Amy-NAcc (lr)	0/32	n/a	+	n/a
4	**F4**	**Amy-NAcc (lr)**	**32/31**	**49–80**	+	+
5	**F4**	**iVTA-NAcc (lr)**	**32/26**	**23–54**	–	–

Note. H = Hypothesis; # Observed/# Required = Number of observed versus number of required consecutively significant ($p = 0.05$) nodes; lr = bilateral; r = right; – = negative; + = positive; ± = bidirectional; bold font = #Observed>#Required.

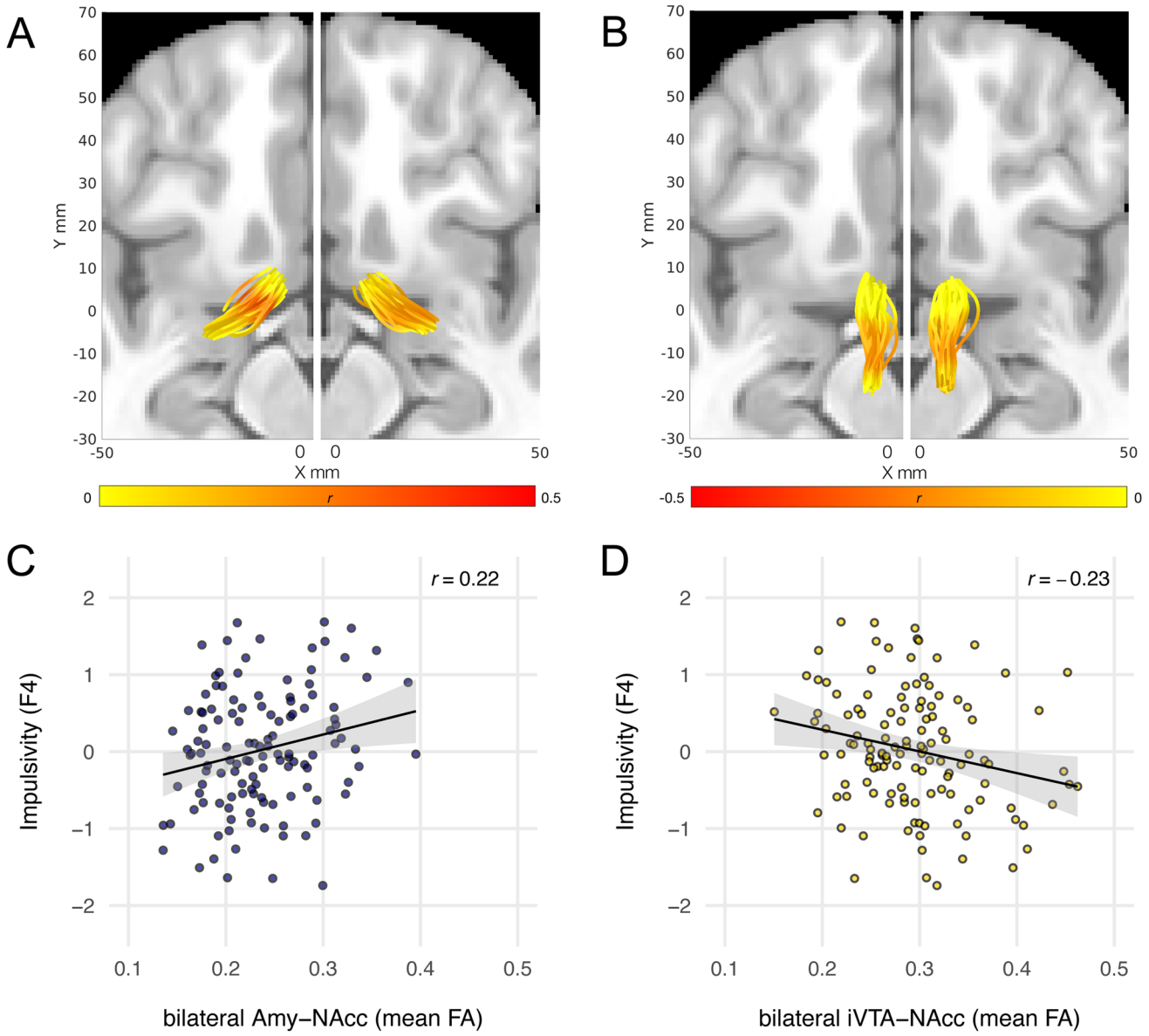

Fig. 3. Association between impulsivity (F4) and FA. (A, B) Group tracts in MNI space with superimposed node-wise associations between impulsivity and FA in left and right Amy-NAcc tract (A), and FA in left and right iVTA-NAcc tract (B). Each tube represents the core trajectory of one participant's tract (in MNI space). Colors indicate node-wise correlation coefficients. (C) Bivariate association between impulsivity and bilateral Amy-NAcc mean FA (calculated from significant nodes shown in panel A). (D) Bivariate association between impulsivity and bilateral iVTA-NAcc mean FA (calculated from significant nodes shown in panel B).

Table 2), and used these in model comparisons. The scatterplots in Figure 3 show the distribution of the resultant summary tract metrics and provide an intuitive visualization of the association between F4 and bilateral Amy-NAcc (panel C) and bilateral iVTA-NAcc (panel D) mean FA. To note, due to the dependence of the summary metrics on the node-wise analyses, the Pearson correlation coefficients reported in panels C and D do not provide unbiased estimates.

To understand whether the two tracts make independent contributions to the impulsivity-capturing factor F4, we performed a set of linear regression models. The results suggest that FA of the Amy-NAcc tract and iVTA-NAcc tract make independent contributions to explaining variance in F4, and that these contributions remain when we control for demographic and methodological covariates (Table 3). Furthermore, specification curve analyses (Fig. S2) supported (a) the robustness of the observed associations between F4 and FA of both Amy-NAcc and iVTA-NAcc projections against the inclusion of exhaustive sets of covariates, and (b) the specificity of the observed results for F4, but none of the other risk preference factors.

Table 3. Linear regression models for impulsivity (F4).

Variable	Demographic	Amy-NAcc	iVTA-NAcc	Combined
Intercept	0.04 (0.09)	0.02 (0.07)	0.02 (0.07)	0.09 (0.09)
Age	-0.12 (0.07)	—	—	**-0.13 (0.07) [-2.01, 0.047]**
Gender (male)	-0.04 (0.14)	—	—	-0.14 (0.14)
Amy-NAcc (nsl)	—	0.02 (0.07)	—	0.01 (0.07)
iVTA-NAcc (nsl)	—	—	0.03 (0.07)	0.07 (0.07)
Amy-NAcc (FA)	—	**0.18 (0.07) [2.56, 0.012]**	—	**0.17 (0.07) [2.47, 0.015]**
iVTA-NAcc (FA)	—	—	**-0.17 (0.07) [-2.54, 0.012]**	**-0.15 (0.07) [-2.11, 0.037]**
AIC	295.07	291.72	291.56	290.12
Adjusted R^2	0.01	0.04	0.04	0.08
RSS (p)	72.55 (0.008)	70.63 (0.035)	70.55 (0.037)	64.94 (—)

Note. Estimates represent standardized regression coefficients. We report the standard error of the estimate in round brackets. For significant variables ($p < 0.05$), we report the exact t-value and p-value in square brackets. Gender was coded with female as the reference category, thus estimates are for males relative to females. nsl = number of streamlines. RSS = residual sum of squares and associated probability (p) for comparison of nested model to full (combined) model. Bold font = $p<0.05$.

Supplementary analyses indicated no effect of interval between the laboratory and MRI session on the main results (Fig. S3).

3.2.3. *Exploratory analyses*

Beyond testing for the hypothesized associations, we also performed exploratory analyses to better understand potential laterality effects (specifically for tracts for which we aggregated tract metrics across hemispheres to test bilateral hypotheses), and to gauge further associations that may present promising starting points for future research (Fig. S4). With regard to laterality, we observed comparably strong effects in left and right hemispheres for the associations between impulsivity and both the iVTA-NAcc and Amy-NAcc tracts. Replicating previous work (MacNiven et al., 2020), supplemental analyses confirmed the anatomical specificity of the link between impulsivity and iVTA-NAcc tract, as no association was observed for the superior tract projecting from the dopaminergic midbrain to the NAcc. Supplementary analyses suggested a strongly lateralized effect of MPFC-NAcc FA on the general risk preference factor R, which we examined further in exploratory supplemental analyses (cf. Supplementary Results). In addition, we observed a lateralized effect of MPFC-NAcc FA for F1, a factor capturing health-related behaviors (Table S3).

4. DISCUSSION

The central question of this research was whether structural characteristics of white-matter fiber tracts converging on the NAcc are associated with individual differences in human risk preference. Previous studies have suggested that functional responses in the NAcc to risk- and reward-related cues can predict real-life risk-taking behavior (Leong et al., 2016; Sherman et al., 2018), account for impulsivity (Buckholtz et al., 2010) and predict drug relapse (MacNiven et al., 2018). Given that NAcc functional activity is driven by neurotransmission from connected brain regions, we hypothesized that DMRI metrics of conNAcctome tracts—including projections from the MPFC, AIns, Amy, and iVTA—may also account for individual differences in risk preference. To counter biased estimates as a result of adopting single, often unreliable risk preference measures (Enkavi et al., 2019; Frey et al., 2017, 2021; Tisdall et al., 2020), here we defined our outcome variables via risk preference factors derived through psychometric modeling in independent research (Frey et al., 2017).

Our results reinforce the notion of the modulatory role played by different projections to the NAcc for specific components of risk preference. Extending previous work (MacNiven et al., 2020) and supporting our prediction, we observed a robust negative association between F4—a factor capturing impulsivity—and FA (as well as 1/RD) of a tract projecting from the dopaminergic midbrain (iVTA) to the NAcc. This link remained when we included demographic and methodological covariates in our analyses, and was specific to a projection traversing below (as opposed to above) the AC (MacNiven et al., 2020). Critically, the observed negative association between impulsivity and iVTA-NAcc FA (and 1/RD) demonstrates generalizability of previous findings (MacNiven et al., 2020; Tisdall et al., 2022) to an independent, non-US sample, thus pointing towards a robust finding in need of a physiological explanation. Regarding their functional role, FA and RD have been shown to capture microstructural

properties (e.g., axon myelination) (Choe et al., 2012; Janve et al., 2013; Leuze et al., 2017, 2021; Ou et al., 2009; Song et al., 2002) of brain tracts, which might affect signal transfer; if higher FA indexes more (coherent) myelination, this could facilitate more efficient or reliable transfer of chemical (e.g., neurotransmitter) and electrical signals between connected brain regions. Suggestive of an endogenous dopamine-related mechanism, prior research has shown that sustained dopamine release in the striatum plays a role in mediating the negative association between dopamine receptor availability in the midbrain and trait impulsivity (Buckholtz et al., 2010); whether iVTA-NAcc tract coherence contributes to this pathway, or supports a separate pathway, requires further research.

Also in line with predictions, and independently of the effect for iVTA-NAcc, Amy-NAcc FA was positively associated with F4 (van den Bos et al., 2014). The 'leakiness' of signal transmission as a function of low coherence could account for this finding. For example, previous work reported a positive association between impulsivity (indexed via temporal discounting) and bilateral connection strength between the amygdala and the striatum (van den Bos et al., 2014), which the authors suggested may have been driven by increased input from the amygdala—computing an incentive value of immediately available options—enhancing the value signal in the striatum.

While these results present a generalization of previous findings (MacNiven et al., 2020) to an independent sample with different demographics, our impulsivity measure was similar to that used in previous work. Specifically, MacNiven et al. (2020) reported iVTA-NAcc FA associations with impulsivity indexed by the Barratt Impulsiveness Scale (BIS) as well as a behavioral measure of impulsivity. The impulsivity factor F4 derived independently by Frey et al. (2017) also exclusively captures variation in BIS. While the bifactor model removed common variance across the battery of risk measures adopted in the BBRS laboratory session from the impulsivity factor, the remaining high positive correlations between F4 and BIS (Fig. S5) suggest that F4 can index BIS. The previously reported association between iVTA-NAcc FA and delay discounting (MacNiven et al., 2020) presents a first hint that this association with impulsivity may extend to alternative impulsivity measures, but further work is required to more systematically examine the convergence of brain-behavior associations across different measures, both within as well as across measurement modalities and domains.

In contrast to our hypotheses concerning the impulsivity-capturing factor F4, we found no support for our predictions concerning associations between the general risk preference factor and bilateral projections from the MPFC, Amy, and right AIns. This discrepancy may be driven by the extent to which (a) different psychometric factors capture specific (cognitive, affective) versus more general, perhaps even strategic processes underlying individual differences (and the reporting thereof), and (b) these processes are subserved by concrete neural substrates like specific brain tracts. For example, to the extent that F4 captures a very specific dimension of risk preference, namely impulse control, the latter has been found to map directly onto (neural markers of) motivation and reward-related mechanisms (Buckholtz et al., 2010; Dalley & Robbins, 2017; Hampton et al., 2017; MacNiven et al., 2020).

Moreover, our exploratory analyses indicated a link between right MPFC-NAcc FA and a domain-specific factor capturing health-related attitudes and behaviors, thus speaking to the utility of examining domain-specific aspects of risk preference, and associations in specific (e.g., clinical) cohorts (Hampton et al., 2019; MacNiven et al., 2020; Morales et al., 2020; Tisdall et al., 2022). Notably, exploratory unilateral analyses also suggested an association between left MPFC-NAcc FA and general risk preference, but given the observed positive effect as opposed to the predicted negative effect, further research is required to replicate the current finding. If replicated, however, this finding could have important implications for extant and future work. For example, fibers between the MPFC and Amygdala have been linked to risk preference (Jung et al., 2018), yet it is possible that these reported fibers actually traverse through the NAcc. In light of our results linking Amy-NAcc projections to impulsivity (rather than general or other domain-specific aspects of risk preference), and exploratory results linking MPFC-NAcc projections to general aspects of risk preference, our results may add anatomical specificity to these previously reported findings.

Our study has some limitations in need of discussion. First, our approach to utilize independently derived risk preference factors aimed to avoid the pitfalls of using single measures with regards to reliability, validity, and convergence (Enkavi et al., 2019; Frey et al., 2017, 2021; Mata et al., 2018; Pedroni et al., 2017). However, this approach raises the question what exactly the resultant factors represent, in particular the general risk preference factor *R*, and how the variance between individuals in this general factor maps onto discrete mechanisms and their neural basis. What is captured by *R* might be the result of many processes, including how individuals integrate aspects such as probability, gains, and losses, as well as modality-specific processes such as how questions are understood and responses generated (note that *R* captures exclusively common variance across self-report measures). Although the cognitive processes underlying the rendering of self-reported risk preference are starting

to become better understood (Steiner et al., 2021), how these are represented in the brain remains to be examined. Moving forward, conceptual clarification of the 'essence' of risk preference (Bringmann et al., 2022) will lie at the heart of progress in our understanding of its neurobiological basis.

Second, the desiderata for the outcome variable equally apply to the predictor(s), the brain markers. A body of work suggests that DMRI metrics are reliable (Kruper et al., 2021; Rokem et al., 2015; Tisdall et al., 2022), relate to microstructural properties (Lazari & Lipp, 2021), and are related to important (clinical) phenotypes (Forkel et al., 2022; Joutsa et al., 2022). However, it is currently still unclear exactly which microstructural properties (e.g., myelination, iron deposition) are captured by metrics such as diffusion coefficients (Lazari & Lipp, 2021; Weiskopf et al., 2021) and how different metrics relate, that is, their convergence. The former will be important to forge ahead with intervention programs targeting specific microstructural properties (Fields, 2015), while the latter will be crucial to efficiently and meaningfully compare results across studies using different tract metrics. For example, our supplementary exploratory analyses suggested no link between impulsivity and fronto-striatal tract structure shown in previous work (Hampton et al., 2017); however, here we used diffusion metrics while previous work computed the number of streamlines to index connectivity strength. To make progress, we need to map the space of common structural metrics and their relationships. To disentangle the role of the molecular, cellular, circuit, and system levels, it will be important to concurrently employ a range of analytical approaches. Fortuitously, advanced neuroscientific methods including tissue clearing (Chung & Deisseroth, 2013) and optogenetic research (Cao et al., 2011) are well poised to provide much-needed answers to questions pertaining to the mapping of metrics to microstructural properties to (behavioral) phenotypes.

Third, in this study, we used data from a cross-sectional sample of healthy young adults, yet the ultimate test will involve examination of the predictive validity of conNAcctome tracts. For this, it will become crucial to harvest existing (large-scale) data sets with longitudinal designs that include repeated scanning sessions, such as the ABCD Study (Casey et al., 2018) or Human Connectome Project (Van Essen et al., 2013). This would also allow researchers to test various theories relating to individual (age) differences in risk preference (Frey et al., 2021; Seaman et al., 2022), potentially even teasing apart the causal mechanisms, such as the effects of socialization and/or selection (Beck & Jackson, 2022). This approach should also be extended to test the predictive validity of biomarkers in different samples, including impulsivity-related outcomes in clinical populations (Karlsson Linnér et al., 2021; Kotov et al., 2018).

5. CONCLUSION

Illuminating the neurobiological basis of individual differences in maladaptive cognition and behavior has the potential for intervention and prevention (Shivacharan et al., 2022), but researchers first need to find reliable indicators for brain markers, outcome measures, and their association. Here, we combined a principled selection of brain tracts with a psychometric assessment of risk preference to provide a first step in this direction for a phenotype that shapes decision making and, consequently, impacts health, wealth, safety, and overall well-being (Moffitt et al., 2011; Steinberg, 2013). Studying the role of the brain, and in particular mapping the generality and specificity of brain markers for risk preference and related constructs, may offer new insights for intervention, and, potentially, prevention.

DATA AND CODE AVAILABILITY

The main analyses reported in this manuscript were preregistered via AsPredicted (https://aspredicted.org/bx49i.pdf). Data and code supporting the main analyses reported in this paper are available on the Open Science Framework (https://osf.io/t27cq/). A preprint version of this manuscript was uploaded to the Open Science Framework (https://osf.io/ab4vr/).

AUTHOR CONTRIBUTIONS

L.T.: Conceptualization, Methodology, Software, Formal analysis, Investigation, Data Curation, Writing—Original Draft, Writing—Review & Editing, Visualization, Project administration, and Funding acquisition. K.M.: Software, Data Curation, Writing—Review & Editing, and Visualization. J.L.: Software, Writing—Review & Editing. R.F.: Methodology, Software, Formal analysis, Investigation, Data Curation, and Writing—Review & Editing. J.R.: Methodology, Writing—Review & Editing, and Funding acquisition. R.H.: Methodology, Writing—Review & Editing, and Funding acquisition. B.K.: Conceptualization, Writing—Review & Editing. R.M.: Supervision, Writing—Review & Editing, and Funding acquisition.

FUNDING

This work was supported by the Swiss National Science Foundation (156172 to R.M., CRSII1_136227 to R.H. and J.R., P2BSP1_188172 to L.T.), and the Max Planck Institute for Human Development, Berlin, Germany.

DECLARATION OF COMPETING INTEREST

The authors declare no conflict of interest.

SUPPLEMENTARY MATERIALS

Supplementary material for this article is available with the online version here: https://doi.org/10.1162/imag_a_00344.

REFERENCES

Alexander, D. C., Dyrby, T. B., Nilsson, M., & Zhang, H. (2019). Imaging brain microstructure with diffusion MRI: Practicality and applications. *NMR in Biomedicine*, *32*(4), e3841. https://doi.org/10.1002/nbm.3841

Appelt, K., Milch, K., Handgraaf, M., & Weber, E. (2011). The decision making individual differences inventory and guidelines for the study of individual differences in judgment and decision-making research. *Judgment and Decision Making*, *6*(3), 252–262. https://doi.org/10.1017/S1930297500001455

Ashburner, J., & Friston, K. J. (2005). Unified segmentation. *NeuroImage*, *26*(3), 839–851. https://doi.org/10.1016/j.neuroimage.2005.02.018

Avants, B. B., Tustison, N. J., Stauffer, M., Song, G., Wu, B., & Gee, J. C. (2014). The Insight ToolKit image registration framework. *Frontiers in Neuroinformatics*, *8*, 1–13. https://doi.org/10.3389/fninf.2014.00044

Aven, T. (2012). The risk concept — Historical and recent development trends. *Reliability Engineering and System Safety*, *99*(0951), 33–44. https://doi.org/10.1016/j.ress.2011.11.006

Aydogan, G., Daviet, R., Karlsson Linnér, R., Hare, T. A., Kable, J. W., Kranzler, H. R., Wetherill, R. R., Ruff, C. C., Koellinger, P. D., BIG BEAR Consortium, & Nave, G. (2021). Genetic underpinnings of risky behaviour relate to altered neuroanatomy. *Nature Human Behaviour*, *5*(6), 787–794. https://doi.org/10.1038/s41562-020-01027-y

Beard, C. L., Schmitz, J. M., Soder, H. E., Suchting, R., Yoon, J. H., Hasan, K. M., Narayana, P. A., Moeller, F. G., & Lane, S. D. (2019). Regional differences in white matter integrity in stimulant use disorders: A meta-analysis of diffusion tensor imaging studies. *Drug and Alcohol Dependence*, *201*, 29–37. https://doi.org/10.1016/j.drugalcdep.2019.03.023

Beck, E. D., & Jackson, J. J. (2022). A mega-analysis of personality prediction: Robustness and boundary conditions. *Journal of Personality and Social Psychology*, *122*(3), 523–553. https://doi.org/10.1037/pspp0000386

Bernoulli, D. (1954). Exposition of a new theory on the measurement of risk. *Econometrica*, *22*(1), 23. https://doi.org/10.2307/1909829

Beshears, J., Choi, J. J., Laibson, D., & Madrian, B. C. (2009). How are preferences revealed? *Journal of Public Economics*, *92*(8–9), 1787–1794. https://doi.org/10.1016/j.jpubeco.2008.04.010

Bringmann, L. F., Elmer, T., & Eronen, M. I. (2022). Back to basics: The importance of conceptual clarification in psychological science. *Current Directions in Psychological Science*, *31*(4), 340–346. https://doi.org/10.1177/09637214221096485

Buckholtz, J. W., Treadway, M. T., Cowan, R. L., Woodward, N. D., Li, R., Ansari, M. S., Baldwin, R. M., Schwartzman, A. N., Shelby, E. S., Smith, C. E., Kessler, R. M., & Zald, D. H. (2010). Dopaminergic network differences in human impulsivity. *Science*, *329*(5991), 532–532. https://doi.org/10.1126/science.1185778

Cao, Z. F. H., Burdakov, D., & Sarnyai, Z. (2011). Optogenetics: Potentials for addiction research. *Addiction Biology*, *16*(4), 519–531. https://doi.org/10.1111/j.1369-1600.2011.00386.x

Cartmell, S. C., Tian, Q., Thio, B. J., Leuze, C., Ye, L., Williams, N. R., Yang, G., Ben-Dor, G., Deisseroth, K., Grill, W. M., McNab, J. A., & Halpern, C. H. (2019). Multimodal characterization of the human nucleus accumbens. *NeuroImage*, *198*, 137–149. https://doi.org/10.1016/j.neuroimage.2019.05.019

Casey, B., Cannonier, T., Conley, M. I., Cohen, A. O., Barch, D. M., Heitzeg, M. M., Soules, M. E., Teslovich, T., Dellarco, D. V., Garavan, H., Orr, C. A., Wager, T. D., Banich, M. T., Speer, N. K., Sutherland, M. T., Riedel, M. C., Dick, A. S., Bjork, J. M., Thomas, K. M., … Dale, A. M. (2018). The Adolescent Brain Cognitive Development (ABCD) study: Imaging acquisition across 21 sites. *Developmental Cognitive Neuroscience*, *32*, 43–54. https://doi.org/10.1016/j.dcn.2018.03.001

Charness, G., Gneezy, U., & Imas, A. (2013). Experimental methods: Eliciting risk preferences. *Journal of Economic Behavior and Organization*, *87*, 43–51. https://doi.org/10.1016/j.jebo.2012.12.023

Choe, A. S., Stepniewska, I., Colvin, D. C., Ding, Z., & Anderson, A. W. (2012). Validation of diffusion tensor MRI in the central nervous system using light microscopy: Quantitative comparison of fiber properties. *NMR in Biomedicine*, *25*(7), 900–908. https://doi.org/10.1002/nbm.1810

Chung, K., & Deisseroth, K. (2013). CLARITY for mapping the nervous system. *Nature Methods*, *10*(6), 508–513. https://doi.org/10.1038/nmeth.2481

Cohen, M. X., Schoene-Bake, J. C., Elger, C. E., & Weber, B. (2009). Connectivity-based segregation of the human striatum predicts personality characteristics. *Nature Neuroscience*, *12*(1), 32–34. https://doi.org/10.1038/nn.2228

Conrod, P. J., O'Leary-Barrett, M., Newton, N., Topper, L., Castellanos-Ryan, N., Mackie, C., & Girard, A. (2013). Effectiveness of a selective, personality-targeted prevention program for adolescent alcohol use and misuse. *JAMA Psychiatry*, *70*(334–342). https://doi.org/10.1001/jamapsychiatry.2013.651

Dalley, J. W., & Robbins, T. W. (2017). Fractionating impulsivity: Neuropsychiatric implications. *Nature Reviews Neuroscience*, *18*(3), 158–171. https://doi.org/10.1038/nrn.2017.8

Dutilh, G., Vandekerckhove, J., Ly, A., Matzke, D., Pedroni, A., Frey, R., Rieskamp, J., & Wagenmakers, E. J. (2017). A test of the diffusion model explanation for the worst performance rule using preregistration and blinding. *Attention, Perception, and Psychophysics*, *79*(3), 713–725. https://doi.org/10.3758/s13414-017-1304-y

Enkavi, A. Z., Eisenberg, I. W., Bissett, P. G., Mazza, G. L., Mackinnon, D. P., & Marsch, L. A. (2019). Large-scale analysis of test— retest reliabilities of self-regulation measures. *Proceedings of the National Academy of Sciences*, *116*(12), 5472–5477. https://doi.org/10.1073/pnas.1818430116

Fields, R. D. (2015). A new mechanism of nervous system plasticity: Activity-dependent myelination. *Nature Reviews Neuroscience*, *16*(12), 756–767. https://doi.org/10.1038/nrn4023

Forkel, S. J., Friedrich, P., Thiebaut de Schotten, M., & Howells, H. (2022). White matter variability, cognition, and disorders: A systematic review. *Brain Structure and Function*, *227*(2), 529–544. https://doi.org/10.1007/s00429-021-02382-w

Frey, R., Pedroni, A., Mata, R., Rieskamp, J., & Hertwig, R. (2017). Risk preference shares the psychometric structure of major psychological traits. *Science Advances*, *3*(10), 1–13. https://doi.org/10.1126/sciadv.1701381

Frey, R., Richter, D., Schupp, J., Hertwig, R., & Mata, R. (2021). Identifying robust correlates of risk preference: A systematic approach using specification curve analysis. *Journal of Personality and Social Psychology*, *120*(2), 538–557. https://doi.org/10.1037/pspp0000287

Haber, S. N., & Knutson, B. (2010). The reward circuit: Linking primate anatomy and human Imaging. *Neuropsychopharmacology*, *35*, 4–26. https://doi.org/10.1038/npp.2009.129

Hampton, W. H., Alm, K. H., Venkatraman, V., Nugiel, T., & Olson, I. R. (2017). Dissociable frontostriatal white matter connectivity underlies reward and motor impulsivity. *NeuroImage*, *150*, 336–343. https://doi.org/10.1016/j.neuroimage.2017.02.021

Hampton, W. H., Hanik, I. M., & Olson, I. R. (2019). Substance abuse and white matter: Findings, limitations, and future of diffusion tensor imaging research. *Drug and Alcohol Dependence*, *197*, 288–298. https://doi.org/10.1016/j.drugalcdep.2019.02.005

Janve, V. A., Zu, Z., Yao, S. Y., Li, K., Zhang, F. L., Wilson, K. J., Ou, X., Does, M. D., Subramaniam, S., & Gochberg, D. F. (2013). The radial diffusivity and magnetization transfer pool size ratio are sensitive markers for demyelination in a rat model of type III multiple sclerosis (MS) lesions. *NeuroImage*, *74*, 298–305. https://doi.org/10.1016/j.neuroimage.2013.02.034

Jbabdi, S., Lehman, J. F., Haber, S. N., & Behrens, T. E. (2013). Human and monkey ventral prefrontal fibers use the same organizational principles to reach their targets: Tracing versus tractography. *Journal of Neuroscience*, *33*(7), 3190–3201. https://doi.org/10.1523/JNEUROSCI.2457-12.2013

Joutsa, J., Moussawi, K., Siddiqi, S. H., Abdolahi, A., Drew, W., Cohen, A. L., Ross, T. J., Deshpande, H. U., Wang, H. Z., Bruss, J., Stein, E. A., Volkow, N. D., Grafman, J. H., van Wijngaarden, E., Boes, A. D., & Fox, M. D. (2022). Brain lesions disrupting addiction map to a common human brain circuit. *Nature Medicine*, *28*(6), 1249–1255. https://doi.org/10.1038/s41591-022-01834-y

Jung, W. H., Lee, S., Lerman, C., & Kable, J. W. (2018). Amygdala functional and structural connectivity predicts individual risk tolerance. *Neuron*, *98*, 394–404.e4. https://doi.org/10.1016/j.neuron.2018.03.019

Kai, J., Khan, A., Haast, R., & Lau, J. (2022). Mapping the subcortical connectome using in vivo diffusion MRI: Feasibility and reliability. *NeuroImage*, *262*, 15. https://doi.org/https://doi.org/10.1016/j.neuroimage.2022.119553

Karlsson Linnér, R., Mallard, T. T., Barr, P. B., Sanchez-Roige, S., Madole, J. W., Driver, M. N., Poore, H. E., de Vlaming, R., Grotzinger, A. D., Tielbeek, J. J., Johnson, E. C., Liu, M., Rosenthal, S. B., Ideker, T., Zhou, H., Kember, R. L., Pasman, J. A., Verweij, K. J. H., Liu, D. J., … Dick, D. M. (2021). Multivariate analysis of 1.5 million people identifies genetic associations with traits related to self-regulation and addiction. *Nature Neuroscience*, *24*(10), 1367–1376. https://doi.org/10.1038/s41593-021-00908-3

Kotov, R., Krueger, R. F., & Watson, D. (2018). A paradigm shift in psychiatric classification: The hierarchical taxonomy of psychopathology (HiTOP). *World Psychiatry*, *17*(1), 24–25. https://doi.org/10.1002/wps.20478

Krosnick, J. A., Judd, C. M., & Wittenbrink, B. (2005). The measurement of attitudes [Section: 2]. In D. Albarracin, B. Johnson, & M. Zanna (Eds.), *The handbook of attitudes* (pp. 21–76). Lawrence Erlbaum Associates Publishers. ISBN: 9781410612823 https://doi.org/10.4324/9781410612823

Kruper, J., Yeatman, J. D., Richie-Halford, A., Bloom, D., Grotheer, M., Caffarra, S., Kiar, G., Karipidis, I. I., Roy, E., & Rokem, A. (2021). Evaluating the reliability of human brain white matter tractometry. *bioRxiv*, 2021.02.24.432740. https://doi.org/10.1101/2021.02.24.432740

Lazari, A., & Lipp, I. (2021). Can MRI measure myelin? Systematic review, qualitative assessment, and meta-analysis of studies validating microstructural imaging with myelin histology. *NeuroImage*, *230*, 117744. https://doi.org/10.1016/j.neuroimage.2021.117744

Leong, J. K., MacNiven, K. H., Samanez-Larkin, G. R., & Knutson, B. (2018). Distinct neural circuits support incentivized inhibition. *NeuroImage*, *178*, 435–444. https://doi.org/10.1016/j.neuroimage.2018.05.055

Leong, J. K., Pestilli, F., Wu, C. C., Samanez-Larkin, G. R., & Knutson, B. (2016). White-matter tract connecting anterior insula to nucleus accumbens correlates with reduced preference for positively skewed gambles. *Neuron*, *89*(1), 63–69. https://doi.org/10.1016/j.neuron.2015.12.015

Leuze, C., Aswendt, M., Ferenczi, E., Liu, C. W., Hsueh, B., Goubran, M., Tian, Q., Steinberg, G., Zeineh, M. M., Deisseroth, K., & McNab, J. A. (2017). The separate effects of lipids and proteins on brain MRI contrast revealed through tissue clearing. *NeuroImage*, *156*, 412–422. https://doi.org/10.1016/j.neuroimage.2017.04.021

Leuze, C., Goubran, M., Barakovic, M., Aswendt, M., Tian, Q., Hsueh, B., Crow, A., Weber, E. M., Steinberg, G. K., Zeineh, M., Plowey, E. D., Daducci, A., Innocenti, G., Thiran, J. P., Deisseroth, K., & McNab, J. A. (2021). Comparison of diffusion MRI and CLARITY fiber orientation estimates in both gray and white matter regions of human and primate brain. *NeuroImage*, *228*, 117692. https://doi.org/10.1016/j.neuroimage.2020.117692

MacNiven, K. H., Jensen, E. L. S., Borg, N., Padula, C. B., Humphreys, K., & Knutson, B. (2018). Association of neural responses to drug cues with subsequent relapse to stimulant use. *JAMA Network Open*, *1*(8), e186466–e186466. https://doi.org/10.1001/jamanetworkopen.2018.6466

MacNiven, K. H., Leong, J. K., & Knutson, B. (2020). Medial forebrain bundle structure is linked to human impulsivity. *Science Advances*, *6*(38), 1–9. https://doi.org/10.1126/sciadv.aba4788

Mamerow, L., Frey, R., & Mata, R. (2016). Risk taking across the life span: A comparison of self-report and behavioral measures of risk taking. *Psychology and Aging*, *31*(7), 711–723. https://doi.org/10.1037/pag0000124

Marek, S., Tervo-Clemmens, B., Calabro, F. J., Montez, D. F., Kay, B. P., Hatoum, A. S., Donohue, M. R., Foran, W., Miller, R. L., Hendrickson, T. J., Malone, S. M., Kandala, S., Feczko, E., Miranda-Dominguez, O., Graham, A. M., Earl, E. A., Perrone, A. J., Cordova, M., Doyle, O., … Dosenbach, N. U. F. (2022). Reproducible brain-wide association studies require thousands of individuals. *Nature*, *603*(7902), 654–660. https://doi.org/10.1038/s41586-022-04492-9

Mata, R., Frey, R., Richter, D., Schupp, J., & Hertwig, R. (2018). Risk preference: A view from psychology. *Journal of Economic Perspectives*, *32*(2), 155–172. https://doi.org/10.1257/jep.32.2.155

Mata, R., Josef, A. K., Samanez-Larkin, G. R., & Hertwig, R. (2011). Age differences in risky choice: A meta-analysis. *Annals of the New York Academy of Sciences*, *1235*(1), 18–29. https://doi.org/10.1111/j.1749-6632.2011.06200.x

Mishra, S. (2014). Decision-making under risk: Integrating perspectives from biology, economics, and psychology. *Personality and Social Psychology Review*, *18*(3), 280–307. https://doi.org/10.1177/1088868314530517

Moffitt, T. E., Arseneault, L., Belsky, D., Dickson, N., Hancox, R. J., Harrington, H., Houts, R., Poulton, R., Roberts, B. W., Ross, S., Sears, M. R., Thomson, W. M., & Caspi, A. (2011). A gradient of childhood self-control predicts health, wealth, and public safety. *Proceedings of the National Academy of Sciences*, *108*(7), 2693–2698. https://doi.org/10.1073/pnas.1010076108

Morales, A. M., Jones, S. A., Harman, G., Patching-Bunch, J., & Nagel, B. J. (2020). Associations between nucleus accumbens structural connectivity, brain function, and initiation of binge drinking. *Addiction Biology*, *25*(3), 1–9. https://doi.org/10.1111/adb.12767

Nichols, T., & Holmes, A. (2002). Nonparametric permutation tests for functional neuroimaging: A primer with examples. *Human Brain Mapping*, *15*(1), 1–25. https://doi.org/10.1002/hbm.1058

Nigg, J. T. (2017). Annual Research Review: On the relations among self-regulation, self-control, executive functioning, effortful control, cognitive control, impulsivity, risk-taking, and inhibition for developmental psychopathology. *Journal of Child Psychology and Psychiatry*, *58*(4), 361–383. https://doi.org/10.1111/jcpp.12675

Ou, X., Sun, S. W., Liang, H. F., Song, S. K., & Gochberg, D. F. (2009). The MT pool size ratio and the DTI radial diffusivity may reflect the myelination in shiverer and control mice. *NMR in Biomedicine*, *22*(5), 480–487. https://doi.org/10.1002/nbm.1358

Pedroni, A., Frey, R., Bruhin, A., Dutilh, G., Hertwig, R., & Rieskamp, J. (2017). The risk elicitation puzzle. *Nature Human Behaviour*, *1*(11), 803–809. https://doi.org/10.1038/s41562-017-0219-x

Poldrack, R. A., Monahan, J., Imrey, P. B., Reyna, V., Raichle, M. E., Faigman, D., & Buckholtz, J. W. (2018). Predicting violent behavior: What can neuroscience add? *Trends in Cognitive Sciences*, *22*(2), 111–123. https://doi.org/10.1016/j.tics.2017.11.003

Rokem, A., Yeatman, J. D., Pestilli, F., Kay, K. N., Mezer, A., van der Walt, S., & Wandell, B. A. (2015). Evaluating the accuracy of diffusion MRI models in white matter. *PLoS One*, *10*(4), e0123272. https://doi.org/10.1371/journal.pone.0123272

Samanez-Larkin, G. R., Levens, S. M., Perry, L. M., Dougherty, R. F., & Knutson, B. (2012). Frontostriatal white matter integrity mediates adult age differences in probabilistic reward learning. *Journal of Neuroscience*, *32*(15), 5333–5337. https://doi.org/10.1523/JNEUROSCI.5756-11.2012

Schonberg, T., Fox, C. R., & Poldrack, R. A. (2011). Mind the gap: Bridging economic and naturalistic risk-taking with cognitive neuroscience. *Trends in Cognitive Sciences*, *15*(1), 11–19. https://doi.org/10.1016/j.tics.2010.10.002

Seaman, K. L., Abiodun, S., Fenn, Z., Samanez-Larkin, G. R., & Mata, R. (2022). Temporal discounting across adulthood: A systematic review and meta-analysis. *Psychology and Aging*, *37*(1), 111–124. https://doi.org/10.1037/pag0000634

Sherman, L., Steinberg, L., & Chein, J. (2018). Connecting brain responsivity and real-world risk taking: Strengths and limitations of current methodological approaches. *Developmental Cognitive Neuroscience*, *33*, 27–41. https://doi.org/10.1016/j.dcn.2017.05.007

Shivacharan, R. S., Rolle, C. E., Barbosa, D. A. N., Cunningham, T. N., Feng, A., Johnson, N. D., Safer, D. L., Bohon, C., Keller, C., Buch, V. P., Parker, J. J., Azagury, D. E., Tass, P. A., Bhati, M. T., Malenka, R. C., Lock, J. D., & Halpern, C. H. (2022). Pilot study of responsive nucleus accumbens deep brain stimulation for loss-of-control eating. *Nature Medicine*, *28*(9), 1791–1796. https://doi.org/10.1038/s41591-022-01941-w

Simonsohn, U., Simmons, J. P., & Nelson, L. D. (2020). Specification curve analysis. *Nature Human Behaviour*, *4*(11), 1208–1214. https://doi.org/10.1038/s41562-020-0912-z

Slovic, P. (1964). Assessment of risk taking behavior. *Psychological Bulletin*, *61*(3), 220–233. https://doi.org/10.1037/h0043608

Song, S. K., Sun, S. W., Ramsbottom, M. J., Chang, C., Russell, J., & Cross, A. H. (2002). Dysmyelination revealed through MRI as increased radial (but unchanged axial) diffusion of water. *NeuroImage*, *17*(3), 1429–1436. https://doi.org/10.1006/nimg.2002.1267

Steegen, S., Tuerlinckx, F., Gelman, A., & Vanpaemel, W. (2016). Increasing transparency through a multiverse analysis. *Perspectives on Psychological Science*, *11*(5), 702–712. https://doi.org/10.1177/1745691616658637

Steinberg, L. (2013). The influence of neuroscience on US Supreme Court decisions about adolescents' criminal culpability. *Nature Reviews Neuroscience*, *14*(7), 513–518. https://doi.org/10.1038/nrn3509

Steiner, M. D., Seitz, F. I., & Frey, R. (2021). Through the window of my mind: Mapping information integration and the cognitive representations underlying self-reported risk preference. *Decision*, *8*(2), 97–122. https://doi.org/10.1037/dec0000127

Stolp, H. B., Ball, G., So, P. W., Tournier, J. D., Jones, M., Thornton, C., & Edwards, A. D. (2018). Voxel-wise comparisons of cellular microstructure and diffusion-MRI in mouse hippocampus using 3D bridging of optically-clear histology with neuroimaging data (3D-BOND). *Scientific Reports*, *8*(1), 1–12. https://doi.org/10.1038/s41598-018-22295-9

Suchting, R., Beard, C. L., Schmitz, J. M., Soder, H. E., Yoon, J. H., Hasan, K. M., Narayana, P. A., & Lane, S. D. (2021). A meta-analysis of tract-based spatial statistics studies examining white matter integrity in cocaine use disorder. *Addiction Biology*, *26*(2), e12902. https://doi.org/10.1111/adb.12902

Tisdall, L., Frey, R., Horn, A., Ostwald, D., Horvath, L., Pedroni, A., Rieskamp, J., Blankenburg, F., Hertwig, R., & Mata, R. (2020). Brain-outcome associations for risk taking depend on the measures used to capture individual differences. *Frontiers in Behavioral Neuroscience*, *14*, 587152. https://doi.org/10.3389/fnbeh.2020.587152

Tisdall, L., MacNiven, K., Padula, C., Leong, J., & Knutson, B. (2022). Brain tract structure predicts relapse to stimulant drug use. *Proceedings of the National Academy of Sciences*, *119*(26), e2116703119. https://doi.org/10.1073/pnas.2116703119

Tournier, J. D., Calamante, F., & Connelly, A. (2007). Robust determination of the fibre orientation distribution in diffusion MRI: Non-negativity constrained super-resolved spherical deconvolution. *NeuroImage*, *35*(4), 1459–1472. https://doi.org/10.1016/j.neuroimage.2007.02.016

van den Bos, W., Rodriguez, C. A., Schweitzer, J. B., & McClure, S. M. (2014). Connectivity strength of dissociable striatal tracts predict individual differences in

temporal discounting. *Journal of Neuroscience*, *34*(31), 10298–10310. https://doi.org/10.1523/JNEUROSCI.4105-13.2014

Van Essen, D. C., Smith, S. M., Barch, D. M., Behrens, T. E., Yacoub, E., & Ugurbil, K. (2013). The WU-Minn Human Connectome Project: An overview. *NeuroImage*, *80*, 62–79. https://doi.org/10.1016/j.neuroimage.2013.05.041

Vul, E., & Pashler, H. (2012). Voodoo and circularity errors. *NeuroImage*, *62*(2), 945–948. https://doi.org/10.1016/j.neuroimage.2012.01.027

Weiskopf, N., Edwards, L. J., Helms, G., Mohammadi, S., & Kirilina, E. (2021). Quantitative magnetic resonance imaging of brain anatomy and in vivo histology. *Nature Reviews Physics*, *3*, 570–588. https://doi.org/10.1038/s42254-021-00326-1

Yarkoni, T. (2009). Big correlations in little studies. Inflated fMRI correlations reflect low statistical power - commentary on Vul et al. (2009). *Perspectives on Psychological Science*, *4*(3), 294–298. https://doi.org/10.1111/j.1745-6924.2009.01127.x

Yeatman, J. D., Dougherty, R. F., Ben-Shachar, M., & Wandell, B. A. (2012). Development of white matter and reading skills. *Proceedings of the National Academy of Sciences*, *109*(44), E3045–E3053. https://doi.org/10.1073/pnas.1206792109

Yeatman, J. D., Dougherty, R. F., Myall, N. J., Wandell, B. A., & Feldman, H. M. (2012). Tract profiles of white matter properties: Automating fiber-tract quantification. *PLoS One*, *7*(11), 1–15. https://doi.org/10.1371/journal.pone.0049790